Radiation Detection Properties of 4H-SiC Schottky Diodes Irradiated Up to 10^{16} n/cm^2 by 1 MeV Neutrons

F. Nava, A. Castaldini, A. Cavallini, P. Errani, and V. Cindro

***Abstract*—We report the results of an experimental study on the radiation hardness of 4H-SiC diodes used as α-particle detectors with 1 MeV neutrons up to a fluence of 8×10^{15} n/cm^2. As the irradiation level approaches the range 10^{15} n/cm^2, the material behaves as intrinsic due to a very high compensation effect and the diodes are still able to detect with a reasonable good Charge Collection Efficiency $(\mathrm{CCE} = 80\%)$. For fluences $> 10^{15}$ n/cm^2 CCE decreases monotonically to $\approx 20\%$ at the highest fluence. Heavily irradiated SiC diodes have been studied by means of Photo Induced Current Transient Spectroscopy (PICTS) technique in order to characterize the electronic levels associated with the irradiation-induced defects. The dominant features of the PICTS spectra occur between 400–700 K; in this temperature range the deep levels associated with the induced defects play the main role in degradation of the CCE. Enthalpy, capture cross-section and concentration of such deep levels were calculated and we found that two deep levels ($\mathrm{E}_t = 1.18$ eV and $\mathrm{E}_t = 1.50$ eV) are responsible for the decrease in CCE. They have been associated to an elementary defect involving a carbon vacancy and to a defect complex involving a carbon and a silicon vacancy, respectively.**

***Index Terms*—DLTS, extended defects, irradiated silicon carbide, PICTS, silicon carbide detectors.**

I. Introduction

CONSIDERING the expected total fluence of fast hadrons above 10^{16} cm^{-2} in a possible upgrade of the Large Hadron Collider (LHC) at CERN to a ten time increased luminosity of 10^{35} cm^{-2} s^{-1}, the semiconductor and/or semi-insulating detectors must be ultra radiation hard providing a fast and efficient charge collection [1].

Silicon carbide is one of the most promising wide band gap material due to its high breakdown electric field, high electron saturation velocity, high operating temperature and high radiation hardness properties [2], [3]. For these reasons over the last few years considerable effort has been concentrated on better understanding the detection performances of silicon carbide detectors after heavy irradiation. The most recent results concern the use of semiconductors epitaxial 4H-SiC [4]–[12] as well as semi-insulating 4H-SiC materials [13]–[15].

It is well known that the degradation of the detectors with irradiation is caused by lattice defects, like creation of vacancies (point-like defects) or damage regions (cluster), independently from the material used for their realization, and, again, that a crucial aspect for the understanding of the defect kinetics at a microscopic level is the correct identification of the crystal defects in terms of their electrical activity. The understanding of the defect kinetics, in fact, would inform how to modify deliberately the material in order to reduce the degradation of the electrical properties of the detectors [16]–[18].

For this purpose a preliminary study has been done by irradiation epitaxial 4H-SiC detectors with 6.5 MeV protons and 8 and 15 MeV electrons [19], [20]; here the study has been extended to the case of 4H-SiC detectors irradiated at different values of 1 MeV neutron fluences up to a maximum value of 8×10^{15} n/cm^2.

II. Detector Fabrication

Tested devices are Schottky diodes manufactured by Selex Integrated Systems (Roma, Italy) on epitaxial 4H-SiC layer grown by CREE Research (USA). The details of the processes are reported elsewhere [21], [22]. The epitaxial layer thickness and its net doping concentration $(\mathrm{N_D} - \mathrm{N_A})$, measured by C/V technique before neutron irradiation, were found to be 39 μm and 6.5×10^{14} cm^{-3}, respectively.

The detector performances, Charge Collection Efficiency (CCE) and Full Width Half Maximum (FWHM), have been measured by 5.486 MeV α-particle from ^{241} Am source in vacuum (about 1Pa), using standard procedures which have been described more in depth elsewhere [23].

The transport properties and the electronic level associated with the defects were analysed by current-voltage (I/V) characteristics, Deep Level Transient Spectroscopy (DLTS) and Photo Induced Current Transient Spectroscopy (PICTS) measurements up to 650 K, respectively.

The free carrier concentration was measured by capacitance-voltage (C/V) characteristics in the as-prepared and the less irradiated ($< 1 \times 10^{14}$ n/cm^2) samples to monitor the compensation effects by intrinsic-irradiation-induced defects. The procedures have been described in the [24].

The samples have been irradiated with increasing fluence of 1 MeV neutrons at the Neutron Irradiation Facility in Ljubljana of the Jozef Stefan Institute. Details about the nuclear reactor

Manuscript received April 26, 2006; revised July 25, 2006. This work was supported by the Istituto Nazionale di Fisica Nucleare (INFN, SICPOS Experiment Groups) and the Ministry of University and Scientific Research (MIUR COFIN 2004). It was performed in the frame work of the CERN RD50 Collaboration.

F. Nava is with INFN, I-40126 Bologna, Italy and Dipartimento di Fisica, Università di Modena e Reggio Emilia, I-41100 Modena, Italy (e-mail: nava@unimo.it).

A. Castaldini, A. Cavallini and P. Errani are with INFN, I-40126 Bologna, Italy and Dipartimento di Fisica, Università di Bologna, I-40127 Bologna, Italy.

V. Cindro is with the Jozef Stefan Institute of Ljubljana, SI-1000 Ljubliana, Slovenia.

Digital Object Identifier 10.1109/TNS.2006.882777

0018-9499/$20.00 © 2006 IEEE

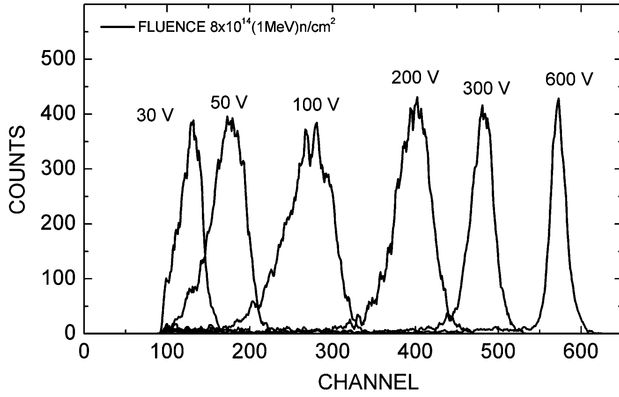

Fig. 1. Response of a 4H-SiC neutron irradiated at 8×10^{14} n/cm^2 detectors to 5.48 MeV ^{241} Am α-particles impinging on the Schottky contact at the indicated applied bias voltage.

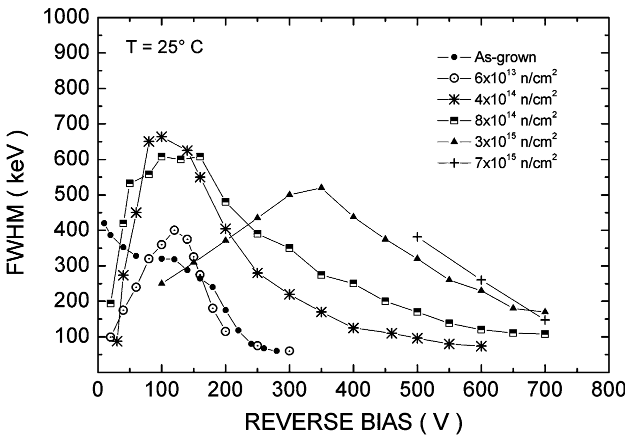

Fig. 2. FWHM as a function of the reverse bias of un-irradiated and neutron irradiated detectors at the indicated fluences.

used (TRIGA), the irradiation set up and procedure and the neutron spectrum can be found in [25], [26].

The neutron irradiation levels used range from 2×10^{13}/cm^2 to 8×10^{15}/cm^2.

III. Experimental Results and Discussion

A. α-Particle Detection

Fig. 1 shows the spectra acquired with a detector irradiated at a fluence of 8×10^{14} n/cm^2 at the indicated reverse bias voltages with a shaping time of 0.5 μs and with the alpha particles impinging the Schottky contact.

The energy resolution measured in keV FWHM is shown in Fig. 2 as a function of the reverse bias for the un-irradiated detectors and, for clearness reason, only for the detectors irradiated at the fluences reported in the inset.

From these curves it can be inferred that the energy resolution evolution shows a maximum (the worst energy resolution case) for the irradiated detectors, while for the un-irradiated one it decreases monotonically with increasing the reverse bias. This behaviour has been already observed in previous works [21], [27], [28] and the reasons why the FWHM shows a maximum, as well as a shift of this maximum, towards higher bias voltages at the highest fluences, are not yet clarified.

Further research is in progress in order to understand these behaviours.

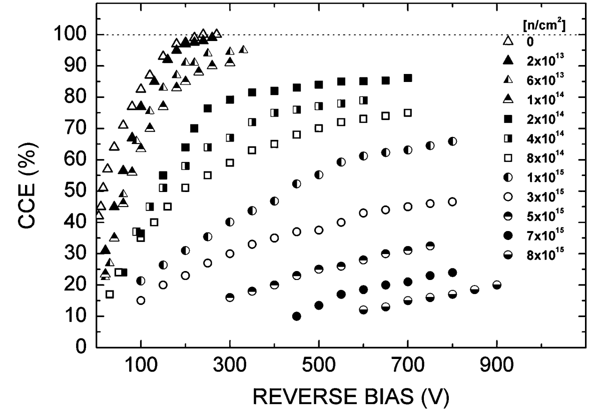

Fig. 3. Experimental charge collection efficiency vs. applied voltage bias for 5.48 MeV α-particles impinging on the Schottky contact of irradiated at different neutron fluences detectors.

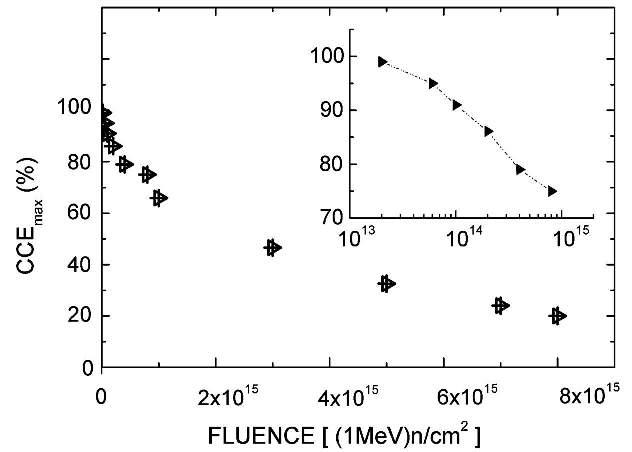

Fig. 4. CCE values at the highest applied voltages, $CCE_{\max}$, as a function of the neutron fluence. In the inset the $CCE_{\max}$ at $\Phi < 10^{15}$ n/cm^2.

Fig. 3 shows the experimental charge collection efficiency (CCE) as a function of the reverse bias for un-irradiated detectors and irradiated ones at the indicated fluences.

The main finding of this analysis are as follows:

i) Irradiated detectors at fluences higher than 2×10^{14} n/cm^2 can withstand higher voltages without breakdown.
ii) The CCE seems to decrease monotonically with increasing the neutron fluence, Φ. This behaviour is well highlighted by plotting the CCE value at the highest reverse bias versus Φ (Fig. 4). The inset evidences this dependence at $\Phi < 10^{15}$ n/cm^2.
iii) Even after a strong irradiation at 8×10^{15} n/cm^2, the detector is still operative, even if the CCE is decreased to about 20%.

B. I/V Curves

The diodes current densities as a function of forward and reverse voltage, before and after irradiation at the more significant neutron fluences, are shown in Fig. 5(a).

From the analysis it can be inferred that:

i) After irradiation the material has become intrinsic and this fact is shown by the decrease of the current density both in forward and reverse bias polarization.

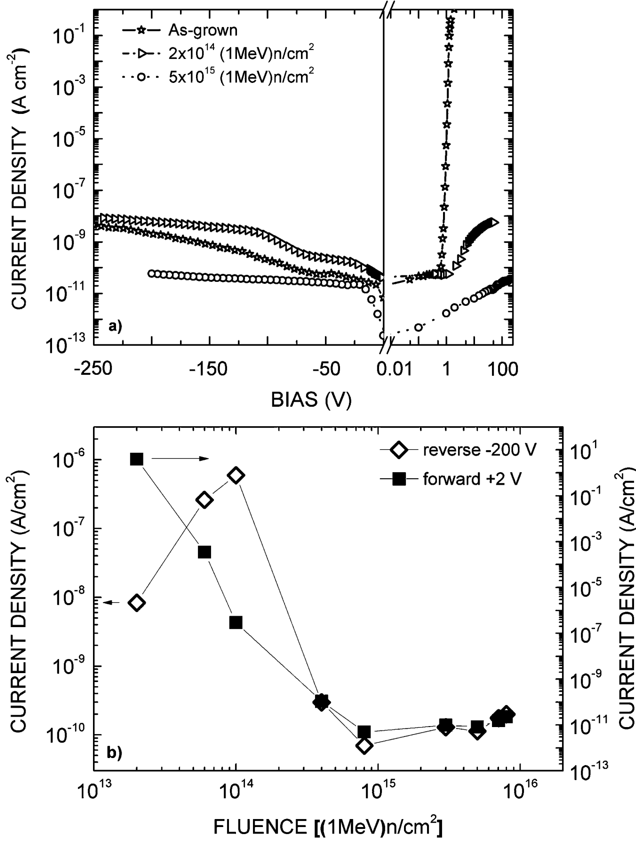

Fig. 5. (a) Forward and reverse current density as a function of the applied bias for un-irradiated and neutron irradiated diodes at 2×10^{14} and 5×10^{15} n/cm^2, respectively. (b) Forward and reverse current density as a function of Φ, measured at $+2$ V and -200 V, respectively.

ii) The irradiation at fluences higher than 8×10^{14} n/cm^2 produces the same current density in both of the bias polarization. Fig. 5(b) shows the forward and reverse current densities as a function of Φ measured at $+2$ V and -200 V, respectively. Such a behaviour has been already observed in previous works concerning the electrical study of electron [24] and neutron [11] irradiated 4H-SiC CVD epitaxial layers and it has been interpreted according to the following model: the un-compensated donor levels in the space charge region are compensated by acceptor-like defects introduced by irradiation in the band-gap with a consequent free carrier concentration decrease. This compensation effect is particularly evident in diodes irradiated at fluences $\geq 10^{14}$ n/cm^2 when the concentration of the induced defects becomes comparable to the net doping density. Since the neutron irradiation expectedly introduces defects in the material, which act as charge carrier trapping centers, a set of reverse current measurements has been done in the temperature range $294 \leftrightarrow 560$ K in order to estimate the thermal activation energies values of the centers.

Fig. 6 shows the Richardson Plot of the reverse diode current I/T ^{2} vs. inverse temperature (1000/T) for un-irradiated and irradiated diodes up to 8×10^{15} n/cm^2. Two approximate grouping of curves, labelled A and B, have been identified which refer to diodes irradiated at fluences lower than 2×10^{14} n/cm^2 and higher than 3×10^{15} n/cm^2, respectively. Nearby each group the range of the thermal activation energy values is reported in eV. The aforesaid grouping has the purpose to suggest an indicative correlation between traps and CCE, that is the remarkable CCE degradation observed in the most irradiated samples has to be ascribed to the induced deepest levels.

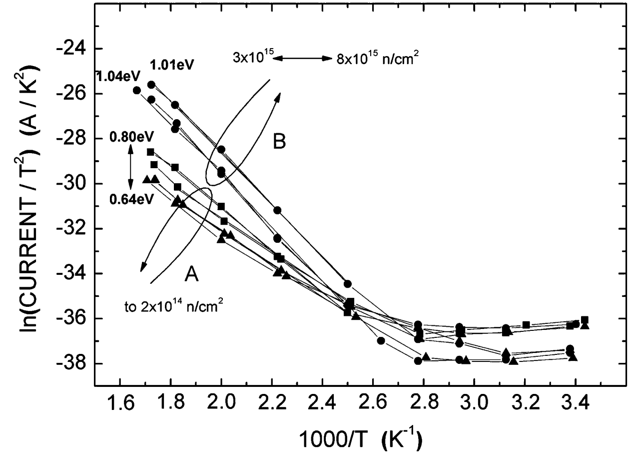

Fig. 6. Richardson Plot for the un-irradiated and neutron irradiated diodes. The thermal activation energy values are indicated nearby the two approximate grouping of curves of the samples, irradiated at the indicated fluences.

C. DLTS and PICTS Analysis

A better electrical characterization of the irradiation-induced defects is however required to monitor in more details the compensation effects and moreover to explain the observed degradation of the CCE at the highest neutron fluences.

For this purpose DLTS and PICTS accurate measurements have been carried out on the as-prepared and neutron irradiated samples.

It is worth reminding that DLTS is used for semiconducting materials and gives information on majority carrier traps, while PICTS is applied to highly resistive samples and gives information on both majority and minority carriers.

It is also to be noted that from DLTS analysis one can determine the trap concentration and from PICTS it is possible to estimate the order of magnitude of the trap density.

Fig. 7(a) shows the DLTS spectrum of the un-irradiated sample with the DLTS signal in the vertical scale converted in the density of levels, $\mathrm{N_t}$, where the levels act as electron trapping centers.

The main finding is that, even if the deep levels SN5 and SN6 likely play the main role in the limitation of the CCE after further irradiation, here their density is too low ($\approx 10^{12}$ cm^{-3}) to effectively influence it, in agreement with the experimental data of Fig. 3.

As a consequence of the neutron irradiation at 2×10^{13} and 6×10^{13} n/cm^2, two main findings can be evidenced from the DLTS results:

i) A new electron trapping center, labelled SN7, with $\mathrm{E_t} = \mathrm{E_c} - 1.50$ eV appears.

ii) $\mathrm{N_t}$ of SN5, SN6 and SN7 increases with the fluence Φ. Their maximum value, however, remains always lower

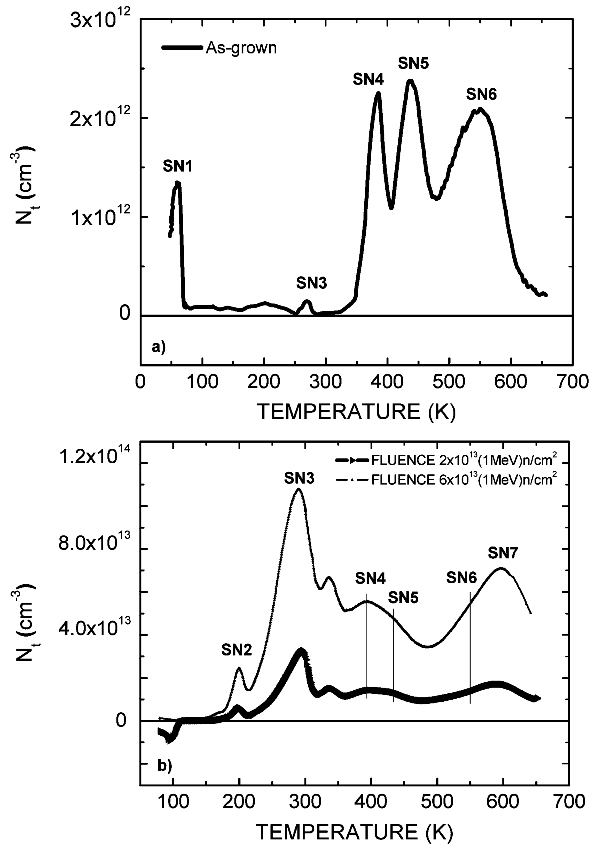

Fig. 7. Typical DLTS spectra of (a) un-irradiated sample and (b) irradiated samples with fluences of 2×10^{13} and 6×10^{13} n/cm^2. They have been obtained with bias voltage -10 V and fill 10 V, pulse width 10 ms and emission rate 11.6 s^{-1}.

than 7×10^{13} cm^{-3}, that explains the good charge collection efficiency (Fig. 3) even after irradiation at the above mentioned fluences.

For this reason DLTS spectra in Figs. 7(a) and (b) have been considered in this study.

The compensation of free charge carriers due to the presence in the gap of defect-related deep levels have been also monitored by C-V characteristics carried out in the temperature range $300 \leftrightarrow 700$ K.

Significant compensation effects were observed mainly in the samples irradiated with fluences higher than 1×10^{14} n/cm^2.

In these samples, because of the high leakage current and other factors related to the low density of free carriers in comparison to the trap density, PICTS was considered the appropriate tool to investigate the microscopic electronic properties of the neutron induced defects, such as enthalpy, $\mathrm{E_t}$, and capture cross section, σ.

With the same technique, the order of magnitude of the defect concentration, $\mathrm{N_t}$, has been obtained using the normalized double-gate signal.

The dependence of the absorbed light on the temperature has been accounted for and its evolution with the fluence has been carefully monitored [29].

The typical shape of a PICTS spectrum, acquired in the temperature range $75 \leftrightarrow 650$ K, is shown in Fig. 8 relevant to a diode irradiated at a fluence of 8×10^{14} n/cm^2.

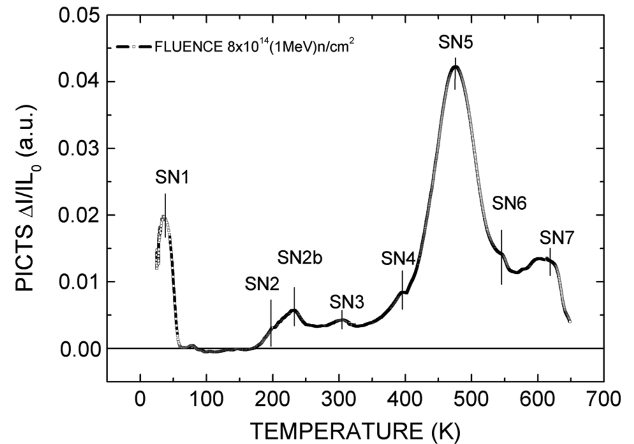

Fig. 8. PICTS spectra acquired with the sample irradiated up to a 1 MeV neutron fluence $\Phi = 8 \times 10^{14}$ n/cm^2 at an emission rate of $\mathrm{e_n} = 25.6$ s^{-1}. The sample was excited by an UV source with a wavelength of 372 nm and polarized at -5 V.

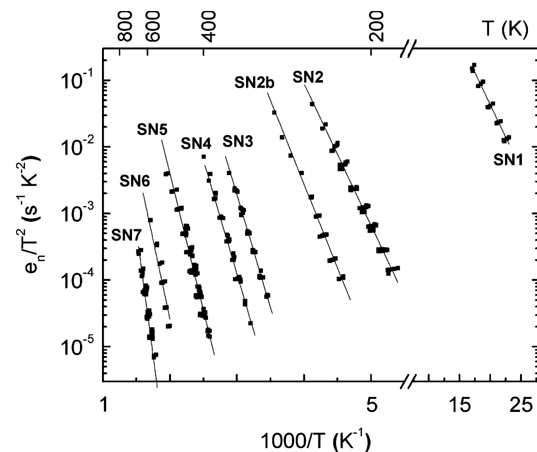

Fig. 9. Arrhenius Plot of the neutron irradiated samples, showing the total detected electron trapping centers together with the temperature ranges required for their detection.

The dominant features occur between 400 and 650 K, excluding SN1.

In this range of temperature broad peaks can be observed which correspond to the deep levels SN5, SN6 and SN7 as it is stressed by the Arrhenius Plot shown in Fig. 9. A few of these levels correspond to the electronic levels detected by DLTS in the lower fluence irradiated samples, but they exhibit different features.

As the fluence rises to higher values ($\Phi > 10^{15}$ n/cm^2), the normalized PICTS signal, Δ I/IL$_0$, of these levels increases and consequently their $\mathrm{N_t}$.

To identify which of them play the main role in the degradation of the detection properties the mean free drift time or trapping time, τ, and the detrapping time, $\mathrm{t_d}$, of these electron trapping centers have been evaluated [7], [42].

$\mathrm{N_t}, \tau$ and $\mathrm{t_d}$ evaluated for the most irradiated samples ($\Phi = 7 \leftrightarrow 8 \times 10^{15}$ n/cm^2) are reported in Table I together with $\mathrm{E_t}$ and their capture cross section σ, determined by the Arrhenius Plot.

Table I reports also the comparison of the levels found in the present work to the levels from literature as well as their possible identification.

TABLE I
ENTHALPY, CONCENTRATION, CAPTURE CROSS SECTION, DETRAPPING, AND TRAPPING TIMES OF THE ELECTRONIC LEVELS OBSERVED IN 4H-SIC SAMPLES IRRADIATED UP TO 1 MEV NEUTRON FLUENCE $\Phi = 7 \leftrightarrow 8 \times 10^{15}$ N/CM^2

						Comparison with published data	
Trap label	E_c-E_t (eV)	N_t (cm^{-3})	σ (cm^2)	Detrapping t_d (sec)	Capture τ (sec)	Level	Attribution
SN1	0.05	10^{14}	8.8×10^{-20}	5.97×10^{-2}	4.99×10^{-3}	**N_{hs}** [a]	$N_{hexag\ site}$
SN2	0.41	10^{14}	3.7×10^{-15}	5.47×10^{-2}	1.40×10^{-7}	**EH1** [b], **$Z_2^{0/+}$** [c]	$V_{Si}^{-/--}$
SN2b	0.49	10^{13}	4.0×10^{-15}	6.82×10^{-2}	1.91×10^{-7}	**RD5, ID_8** [d], **$Z_1^{0/+}$** [c]	-
SN3	0.68	10^{13}	7.0×10^{-15}	1.17×10^{-1}	1.20×10^{-7}	**Z1/Z2** [e c]	$V_{Si}+V_C$
SN4	0.68	-	6.0×10^{-16}	-	-	**M2** [f], **EH3** [b]	-
SN5	0.82	10^{15}	2.0×10^{-16}	3.94×10^{-3}	7.61×10^{-6}	**$RD_{1/2}$** [d], **SI5** [g]	V_{Si}^{+}
SN6	1.16	10^{15}	2.8×10^{-15}	1.02×10^{-1}	4.95×10^{-9}	**EH5** [b], **$IL_{4/5}$** [h]	$Vc+V_{Si}$
SN7	1.50	10^{16}	3.0×10^{-14}	8.56×10^{-2}	3.42×10^{-11}	**EH6/EH7** [b i]	Vc^{+}, Vc^{+}complex

a) [30], [31], [32] **b)** [33] **c)** [34] **d)** [35], [36] **e)** [37] **f)** [38] **g)** [39] **h)** [40] **i)** [41]

It is obvious that the deepest levels SN6 and SN7 become dominant at the highest fluence, meaning that their trapping times are comparable to or lower than the transit time of the electrons in the detector and that their detrapping times are much higher than the time constant (5×10^{-7} s) of the shaping network, which defines the time the electronic system will spend collecting any charge induced by the ionising radiation. In fact, at the highest reverse bias, electrons require about 2×10^{-10} s to drift the SiC detector depleted region (39 μm) at the saturation drift velocity of 2×10^{7} cm/s. In these cases the most of generated charge carriers are lost and do not contribute to the collected charge signal [42].

It is worth noting that it is not possible to quantitatively assess the dependence of N_t on Φ for the levels SN6 and SN7 when Φ goes up to values higher than 3×10^{15} n/cm^2.

On other hand, because of the considerable importance of these centers, we are aware that what is required to a quantitative analysis is a study carried out with a more appropriate technique, such as the Current-Deep Level Transient Spectroscopy (I-DLTS) [43], which we are currently setting up and we hope to carry out on these samples in the near future.

IV. CONCLUSION

Radiation hardness after 1 MeV neutron fluences in the range $10^{13} \leftrightarrow 10^{16}$ n/cm^2 of 4H-SiC Schottky diodes has been analysed. The main findings of this analysis are the following:

i) Even after an irradiation at fluence of 8×10^{15} n/cm^2, the diodes were still able to detect alpha particles of a ^{241} Am source with a CCE of about 20% at the highest reverse bias applied.

ii) The detectors continue to be operative with a high CCE ($\approx 80\%$) until fluences of the order of some 10^{14} n/cm^2. After fluences of the order of 10^{15} n/cm^2, the collected charge signal decreases with a decreasing rate of degradation.

iii) A change of the material to intrinsic has been observed with a flat C-V response and with very similar I-V response in forward and reverse bias as the irradiation levels approaches the range 10^{15} n/cm^2. Moreover for irradiated samples the leakage current remain very low in the range $10^{-10} \leftrightarrow 10^{-11}$ A/cm^2, even after fluences of the order of 10^{16} n/cm^2. Actually the material is behaving as intrinsic because it is highly compensated. Compensation of 4H-SiC Schottky diodes due to radiation induced defects has been already reported [24].

iv) According to I-V measurements as a function of temperature (Richardson Plot), we expect that the trapping centers, which play the main role in the decrease of the CCE, are related to deep levels with $E_t > 1.04$ eV.

v) PICTS measurements, carried out on samples irradiated at $\Phi > 1 \times 10^{14}$ n/cm^2, confirm this expectation. PICTS spectra exhibit, in fact, broad and distorted peaks in the temperature range $T = 400 - 700$ K, which increase in amplitude with Φ. They are defects, which behave as electron trapping centers and have been electrically characterized in terms of enthalpy (E_t), cross section and, even if only in order of magnitude, concentration (N_t). Two of these defects, for whom N_t was calculated to be in the order of $10^{15} \leftrightarrow 10^{16}$ cm^{-3} for the most irradiated samples, have been identified as the trapping centers, which play the main role in the degradation of the detector's response. They are, indeed, deep levels with $E_t = 1.16$ and 1.50 eV, respectively and, above all, with trapping times comparable or lower than the transit time of the charge carriers. According to the data reported in literature [33], [40], [41], these defects can be identified as a defect complex involving carbon vacancy, V_c, and carbon and silicon vacancy, $V_c + V_{si}$.

ACKNOWLEDGMENT

C. Lanzieri and S. Lavanga of Selex-SI (Roma-Italy) are acknowledged for the diodes realization.

REFERENCES

[1] M. Bruzzi and M. Michel, RD-50 Status Rep. 2002/2003 CERN-LHCC-2003-058 and LHCC-RD-002.
[2] *Silicon Carbide High Temperature Integrated and Sensors*, [Online]. Available: http://www.grc.nasa.gov/WWW/SiC.html
[3] *IEEE Trans. Electro. Devices*, vol. 45, Mar. 1999, number dedicated to silicon carbide.

[4] A. R. Dulloo *et al.*, "Simultaneous measurements of neutron and gamma-ray radiation levels from a TRIGA reactor core using silicon carbide semiconductor detectors," *IEEE Trans. Nucl. Sci.*, vol. 46, no. 3, pp. 275–279, Jun. 1999.

[5] S. Seshadri *et al.*, "Demonstration of a SiC neutron detector for high-radiation environments," *IEEE Trans. Nucl. Sci.*, vol. 46, no. 3, pp. 567–571, Mar. 1999.

[6] F. Nava *et al.*, "Radiation tolerance of epitaxial silicon carbide detectors for electrons, protons and gamma-rays," *Nucl. Instrum. Methods Phys. Res. A*, vol. A505, p. 645, 2003.

[7] F. Nava *et al.*, "Charged particle detection properties of epitaxial 4H-SiC Schottky diodes," *Mater. Sci. Forum*, vol. 353–356, p. 757, 2001.

[8] E. Kalinina *et al.*, "Comparative study of 4H-SiC irradiated with neutrons and heavy ions," *Mater. Sci. Forum*, vol. 483–485, pp. 377–380, 2005.

[9] A. Castaldini *et al.*, "Electronic levels induced by irradiation in 4H-silicon carbide," *Mater. Sci. Forum*, vol. 483–485, pp. 359–364, 2005.

[10] A. M. Strel'chuck *et al.*, "Influence of gamma-ray and neutron irradiation on injection characteristics of 4H-SiC pn structures," *Mater. Sci. Forum*, vol. 483–485, pp. 993–996, 2005.

[11] E. Kalinina *et al.*, "Electrical study of fast neutron irradiated devices based on 4H-SiC CVD epitaxial layers," *Mater. Sci. Forum*, vol. 457–460, pp. 705–708, 2004.

[12] P. J. Sallin and J. Vaitkus, "New materials for radiation hard semiconductor detectors," *Nucl. Instrum. Methods Phys. Res. A*, vol. A557, p. 479, 2006.

[13] M. Rogalla *et al.*, "Particle detectors based on semi-insulating silicon carbide," *Nucl. Phys.*, vol. B78, p. 516, 1999, (proc. suppl.).

[14] W. Cunningham *et al.*, "Performance of irradiated bulk SiC detectors," *Nucl. Instrum. Methods Phys. Res. A*, vol. A509, p. 127, 2003.

[15] J. Grant *et al.,* in *6th Int. Work Rad. Imag. Detectors IWORID-2004*, Glasgow, Scotland [Online]. Available: http://www.iworid2004.ph.gla.ac.uk/pages/prog.html

[16] *CERN RD48 Collaboration*, [Online]. Available: http://rd48.web.cern.ch/rd48/

[17] G. Lindstrom *et al.*, "The ROSE Collaboration," *Nucl. Instrum. Methods Phys. Res. A* vol. A466, p. 308, 2001 [Online]. Available: http://rd48.web.cern.ch/rd48/

[18] D. Menichelli *et al.*, "PICTS analysis of extended defects in heavily irradiated silicon," *IEEE Trans. Nucl. Sci.*, vol. 49, no. 5, p. 2431, Oct. 2002.

[19] A. Castaldini *et al.*, "Deep levels by proton and electron irradiation in 4H-SiC," *J. Appl. Phys.*, vol. 98, 2005.

[20] G. Alfieri *et al.*, "Capacitance spectroscopy study of high electron irradiated and annealed 4H-SiC," *Mater. Sci. Forum*, vol. 483–485, pp. 365–368, 2005.

[21] F. Nava *et al.*, "Minimum ionizing and alpha particles detectors based on epitaxial semiconductor silicon carbide," *IEEE Trans. Nucl. Sci.*, vol. 51, no. 1, pp. 238–244, Feb. 2004.

[22] S. Sciortino *et al.*, "Effect of heavy proton and neutron irradiation on epitaxial 4H-SiC Schottky diodes," *Nucl. Instrum. Methods Phys. Res. A*, vol. A552, p. 138, 2005.

[23] F. Nava *et al.*, "Investigation of Ni/4H-SiC diodes as radiation detectors with low doped n-type 4H-SiC epilayers," *Nucl. Instrum. Methods Phys. Res. A*, vol. A510, p. 273, 2003.

[24] A. Castaldini *et al.*, "Low temperature annealing of electron irradiation induced defect in 4H-SiC," *Appl. Phys. Lett.*, vol. 85, p. 3780, 2004.

[25] M. Ravnick and R. Jeraj, "Research reactor benchmarks," *Nucl. Sci. Eng.*, vol. 145, p. 145, 2003.

[26] D. Zontar *et al.*, "Time development and flux dependence of neutron-irradiation induced defects in silicon pad detectors," *Nucl. Instrum. Methods Phys. Res. A*, vol. A426, p. 51, 1999.

[27] C. Manfredotti *et al.*, "Investigation of 4H-SiC Schottky diodes by ion beam induced charge (IBIC) technique," *Appl. Surf. Sci.*, vol. 184, p. 448, 2001.

[28] F. Nava *et al.*, "Radiation tolerance of epitaxial silicon carbide detectors for electrons and γ-rays," *Nucl. Instrum. Methods Phys. Res. A*, vol. A514, p. 126, 2003.

[29] M. Tapiero *et al.*, "Photoinduced current transient spectroscopy in high-resistivity bulk materials: Instrumentation and methodology," *J. Appl. Phys.*, vol. 64, no. 8, pp. 4006–4012, 1988.

[30] A. O. Evwaraye *et al.*, "Shallow and deep levels in n-type 4H-SiC," *J. Appl. Phys.*, vol. 79, no. 10, pp. 7726–7730, 1996.

[31] T. Kimoto *et al.*, "Nitrogen donors and deep levels in high-quality 4H-SiC epilayers grown by chemical vapor deposition," *Appl. Phys. Lett.*, vol. 67, no. 19, pp. 2833–2835, 1995.

[32] A. A. Lebedev *et al.*, "Deep level centers in silicon carbide," *Semicond.*, vol. 33, no. 2, pp. 107–130, 1999.

[33] L. Storasta *et al.*, "Deep levels created by low energy electron irradiation in 4H-SiC," *J. Appl. Phys.*, vol. 96, no. 9, pp. 4909–4915, 2004.

[34] C. G. Hemmingsson *et al.*, "Negative-U centers in 4H silicon carbide," *Phys. Rev.*, vol. B58, no. 16, 1998, R1.

[35] T. Dalibor *et al.*, "Deep defect centers in silicon carbide monitored with deep level transient spectroscopy," *Phys. Stat. Sol. (a)*, vol. 162, p. 199, 1997.

[36] L. Storasta *et al.*, "Proton irradiation induced defects in 4H-SiC," *Mater. Sci. Forum*, vol. 353–356, pp. 431–434, 2001.

[37] A. Castaldini *et al.*, "Assessment of intrinsic nature of deep level Z1/Z2 in proton irradiated 4H-SiC by compensation defects," *Semicond. Sci. Technol.*, vol. 21, p. 724, 2006.

[38] D. M. Martin *et al.*, "Bistable defect in mega-electron-volt proton implanted 4H silicon carbide," *Appl. Phys. Lett.*, vol. 84, p. 1704, 2004.

[39] N. T. Son *et al.*, "Defect in semi-insulating SiC substrates," *Mater. Sci. Forum*, vol. 433–436, p. 45, 2003.

[40] St. G. Muller *et al.*, "Sublimation-grown semi-insulating SiC for high frequency devices," *Mater. Sci. Forum*, vol. 433–436, pp. 39–44, 2003.

[41] Y. Negoro *et al.*, "Stability of deep centers in 4H-SiC epitaxial layers during thermal annealing," *Appl. Phys. Lett.*, vol. 85, no. 10, pp. 1716–1718, 2004.

[42] M. Martini, J. W. Mayer, and K. Zanio *et al., Appl. Solid State Sci.*, Wolfe, Ed. New York: Academic, 1972, vol. 3.

[43] Z. Li, "Systematic modelling and comparisons of capacitance and current-based microscopic defect analysis techniques for measurements of high-resistivity silicon detectors after irradiation," *Nucl. Instrum. Methods Phys. Res. A*, vol. A403, pp. 399–416, 1998.